

# On the Influence of the Propagation Channel in the Performance of Energy-Efficient Geographic Routing Algorithms for Wireless Sensor Networks (WSN)

P. Padilla · J. Camacho · G. Maciá-Fernández ·  
J. E. Díaz-Verdejo · P. García-Teodoro · C. Gómez-Calero

© Springer Science+Business Media, LLC. 2012

**Abstract** In this paper, the influence of the features of the propagation channel in the performance of energy-efficient routing algorithms for wireless sensor networks is studied. Although there are a lot of works regarding energy-efficient routing protocols, almost no reference to realistic propagation channel models and influence is made in the literature. Considering that the propagation channel may affect the efficiency of the different energy-efficient routing algorithms, different propagation scenarios are proposed in this work, from the most simplistic free-space propagation model to more complex ones. The latter includes the effects of multipath propagation, shadowing, fading, etc. In addition, spatial diversity transmission/reception models are considered to mitigate the effects of hard propagation fading. Some results are provided comparing the performance of several energy-efficient routing algorithms in different scenarios.

**Keywords** Energy-efficient routing · Wireless sensor networks · Propagation channel

## 1 Introduction

There is a growing interest in wireless sensor networks (WSN), as the demand for communications services in very diverse scenarios is increasing. WSN deployment is being enhanced by the necessity of providing more and more adapted solutions, in terms of autonomous support for a variety of potential applications. Advances in technology and low-power consumption devices have turned WSNs into one of the most versatile solutions for the deployment of ad-hoc communication networks. Simple tiny communication devices with power autonomy,

---

P. Padilla (✉) · J. Camacho · G. Maciá-Fernández · J. E. Díaz-Verdejo · P. García-Teodoro  
Signal Theory, Telematics and Communications Department, CITIC, University of Granada, Granada,  
Spain  
e-mail: pablopadilla@ugr.es

C. Gómez-Calero  
Radiation Group, Signal, Systems and Radiocommunications Department,  
Technical University of Madrid, Madrid, Spain

low-powered microprocessors and versatile functions constitute the core of WSNs and their interest. Such features, combined with a large amount of possible applications and scenarios with a significant number of sensor nodes, have provided many challenges to the design and management of WSN.

The physical and link layers are fundamental in the development of all kind of sensor applications and different issues concerning them have been deeply studied [1]. Many efforts have been applied to research on these areas, considering WSN power awareness, node processing, efficient radio communication hardware, low duty cycle, energy-aware MAC protocols, etc. so that the entire power consumption of the different nodes and the network itself is minimized. At the network layer, the main target is to find energy-efficient transmission routes and reliable transmission of data from the sensor nodes to the destination so that the lifetime of the devices in the network is maximized. The global power consumption and its distribution in the different nodes depend on the nature of the communication within a particular network. For instance, in monitoring sensor networks the data typically flow from the different nodes towards some of them that concentrate data traffic and whose role in the network is vital. This situation is in contrast with other cases, where the contribution of each node to the network is similar and the network topology may be quite flexible, depending on the requirements at each moment [2]. Depending on the network topology there are a variety of different routing algorithms, proposed for different traffic flow distributions through the network [3].

As mentioned, energy saving and low power consumption is a key concern in WSNs. In general, it is considered that the nodes that constitute the network are small autonomous devices distributed in whatever kind of scenario for a variety of applications and purposes [1,4,5]. In many cases, the particular features of these smart scenarios require the usage of batteries and limited power supply for the network nodes. Typically, the existing limitations in WSN nodes prevent from storing the complete topology of the network and transmission routes at each node. In contrast to best-route-like routing algorithms, energy-efficient routing algorithms only consider the direct neighbor list in any node and select one of them to be the next hop in the route, being all operations purely local. In this situation, every node tracks its direct neighbors and keeps their location information in order to forward packets. Thus, the state stored in each node is reduced, with no requirement for the establishment or maintenance of a route. As a result, such algorithms conserve energy and bandwidth, since discovery-packet strategies and node-state propagation are not required beyond a single hop. Each node knows his location and the locations of the neighbors are typically learned via one-hop broadcast, while the location of the destination is obtained by means of a so called location service [6] either via GPS or through network localization techniques [7]. These nodes whose location is a reference within the complete network are called *anchors* [8]. Under these circumstances, each node selects the next forwarding node only based on the location of itself, its neighbors and the ultimate destination.

The environment and its propagation features are also an issue of great concern in WSN. Some experiences [7,9] have revealed that the communications in WSN can experiment unacceptable degradation, making the network fairly unreliable. This situation forces the deviation of the performance in the network to a large extent from the idealized perfect-reception-within-range models commonly used to evaluate the WSN performance. Most of the proposed geographic routing algorithms commonly employ distance-based forwarding techniques that work properly in ideal conditions. However, such techniques may degrade their performance in realistic conditions.

There is a lot of literature regarding energy efficient routing algorithms [7,11–18]. However, the propagation scenarios considered in most of them are usually based on simplified

propagation models, not taking into account the possible influence of the propagation channel and its possible degradation effects in the performance of such algorithms. A variety of works propose new algorithms for energy-efficient routing, but they consider a simplistic propagation model based only in Friis' propagation equation [7, 11–15, 17, 19, 20]. There are also relevant articles attending to different important circumstances such as relative uncertainty in the node position [7], border effect [12], or other complex situations [13], not considering again propagation issues and their influence. What is more, there are articles that center part of the attention on the physical layer, but although the propagation models are a bit more elaborated, important effects such as fading or shadowing remain unattended [21]. Finally, almost no reference is found regarding energy-efficient routing algorithms and propagation channel techniques [spatial diversity, multiple input multiple output (MIMO), etc.] to overcome the hard effects of channel degradation in problematic propagation scenarios.

The main contribution of this work is to point out the necessity of considering realistic scenarios for the proper evaluation of the energy-efficient routing algorithms and whatever issue related to them. Thus, in this work, it is illustrated the performance of some of the most popular energy-efficient routing algorithms in realistic environments regarding the propagation channel and its real features. The manuscript is organized as follows: in Sect. 2, several energy-efficient geographic routing algorithms are summarized, along with their particular features. Section 3 is devoted to propagation issues concerning the different propagation scenarios considered. Section 4 offers an overview of the performance of the routing algorithms in the proposed propagation scenarios. Eventually, in Sect. 5, conclusions are drawn.

## 2 Energy-Efficient Geographic Routing Algorithms

A variety of energy-efficient routing algorithms have been proposed in the literature [7, 10, 11]. The power consumption along the transmission route and its relation with the number of hops is essential to evaluate which routing algorithm offers the best performance in any WSN network. Considering also the fraction of power consumption in any node not only due to transmission ( $P_{Tx}$ ) but also to node functioning and processing ( $P_{elec}$ ), it can be noticed that the best choice in terms of used power in each hop does not lead necessarily to the most energy efficient route. The number of hops and node consumption are key factors to compute the global energy consumption within a WSN. In some cases, increasing the hop-count (decreasing hop-distance as a consequence) may result in the reduction of the total power consumption. In other cases, the node consumption  $P_{elect}$  may be the dominant term in the total node consumption, not leading to the most energy efficient route.

Some of the most popular algorithms evaluated in this work are described in what follows. Please refer to Fig. 1 for the notation. For each node, the zones  $A_{IN}$  and  $A_{OUT}$  are defined by  $d_{opt}$ , which is defined as the value in which the relation between the distance covered and the needed power reach its optimum. The computation of  $d_{opt}$  is actually an optimization problem considering the propagation losses of the scenario and the node consumption. If the relation  $s$  between the covered distance in any hop ( $d_{ij}$ ) and the total needed power is defined,  $d_{opt}$  can be found as follows:

$$s = \frac{d_{ij}}{P_{Tx_{ij}} + 2P_{elect}} \rightarrow \frac{\partial s}{\partial d_{ij}} = 0 \rightarrow d_{opt} \quad (1)$$

The equation for  $d_{opt}$  is provided in Table 1 (see ‘‘Appendix’’ for more details).  $FTS$  is the forward transmission sector of the source node, defined to guarantee the advance of the transmission towards the destination node, avoiding loops or divergent routes. This sector is

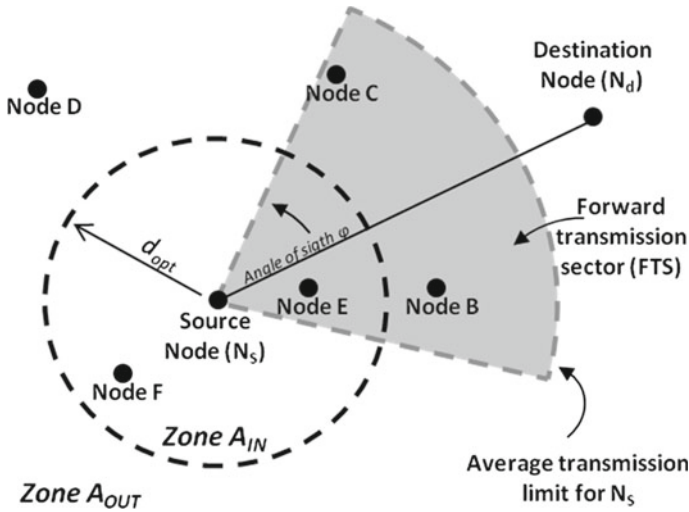


**Fig. 1** Node topology description and nomenclature for the description of the different routing algorithms

**Table 1** Simulation scenario description

<i>Sensor node features</i>	
Sensor type	MICAz
Working frequency	2.4 GHz
Transmission rate	250 Kbps
Sensitivity (sens)	-94 dBm (typ)
$P_{Tx}$	0 dBm (max)
Node consumption	RF chain: Tx = 11–17 mA (-17.8–15 dBW) Rx = 19.6 mA (-14.5 dBW) Sleep = 1 $\mu$ A (-57.5 dBW) Processing: ~8 mA (-18.4 dBW)
Coverage (max)	35–100 m
Tx/Rx antenna	Dipole antenna, Gmax = 2 dBi, Gmin = 1.8 dBi
<i>Wireless sensor network features</i>	
Topology	2D (x, y) square grid node distribution. $N_s$ at (0, 0) and $N_d$ at (300, 300)
Dimensions	300 $\times$ 300 m
Number of nodes	Variable: 2–350 nodes
Node distribution	Uniform node distribution in the (x, y) grid
$d_{opt}$	$d_{opt} = \sqrt[n]{\frac{2P_{elect}\lambda^2}{4\pi^2 d_0^{(2-n)}(n-1)} \frac{S}{8T_x 8R_x}}$

defined by an angle of sight  $\pm\varphi$  around the axis formed by the source and the destination node.  $N_s$  and  $N_d$  are the source and the destination nodes, respectively. Among the available energy-efficient algorithms, some of the most popular ones are selected and evaluated in this work:

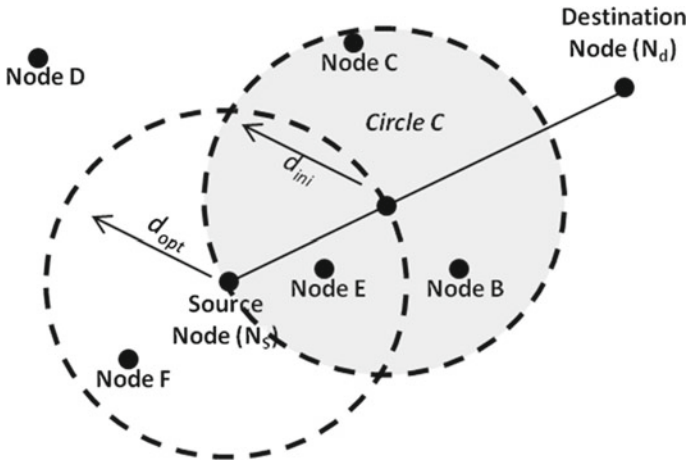


**Fig. 2** Node topology description and nomenclature for the *EEGR* algorithm

- **Greedy Minimum Energy [7]:** At any hop, the next relay is set to the node in *FTS* that is closest to the source node of the hop,  $N_s$ .
- **Bounded Distance from Above (*B\_Above*) [7, 10]:** At any hop, if  $N_d$  is in zone  $A_{IN} \cap FTS$ , then the source node ( $N_s$ ) transmits to  $N_d$  directly, otherwise pick as the next relay the node in  $A_{OUT} \cap FTS$  that is closest to  $N_s$ .
- **Bounded Distance from Below (*B\_Below*) [7, 10]:** At any hop, if  $N_d$  is in  $A_{IN} \cap FTS$ , then  $N_s$  transmits to  $N_d$  directly, otherwise it picks, as the next relay, the node in  $A_{IN} \cap FTS$  that is furthest from  $N_s$ . If such a node does not exist, apply *Bounded Distance from Above*.
- **Modified Geographic Random Forwarding (*GeRaF*) [15]:** At any hop, pick, as the next relay, the node that is closest to the destination, among those close to the ring with center in  $N_s$  and coverage radius  $d_{opt}$ . If no such a node exists, apply the *Bounded Distance from Above* algorithm.
- **Modified Energy-Efficient Geographic Routing (*EEGR*) [20]:** At any hop, consider the line from the current relay to the destination  $N_d$ , pick the point on this line at a distance  $d_{opt}$  from the current relay. Trace the circle *C* of radius  $d_{opt}$  (see Fig. 2). Consider all the nodes within the circle. If  $N_d$  is in the circle, transmit directly to it; else transmit to the closest node to  $N_d$  of the circle.

In order to have a reference power level, the most efficient route in terms of lowest global power consumption is also computed by means of the Dijkstra algorithm. This case is treated here to compare the performance of the routing algorithms with a threshold reference value. However, it is not as a possible choice because the routing decision has to be local at each node and the best-route approach implies, at each node of the network, a precise global knowledge of the rest of the nodes and the exact amount of power (due to propagation losses, fading, etc.) to reach each one.

### 3 The Propagation Channel

The conventional free space propagation model assumes the evolution of the losses level with distance as:

$$P_{R_x}(d) = P_{T_x} + G_{T_x} + G_{R_x} + 20 \log \left( \frac{\lambda}{4\pi d_0} \right) + 10 \log \left( \frac{d_0}{d} \right) \quad (2)$$

where  $P_{R_x}$  and  $P_{T_x}$  make reference to the received and transmitted power,  $\lambda$  is the signal wavelength,  $d$  is the distance between the receiver and the transmitter,  $G_{T_x}$  and  $G_{R_x}$  are the antenna gains on the transmitter and receiver, respectively,  $d_0$  is the reference distance in which losses evolution are well known (e.g.  $d_0 = 1$  m in indoor scenarios), and  $n$  is the attenuation coefficient considered from  $d_0$  and beyond. The value of  $n$  depends on the scenario considered (indoor or outdoor) and its nature (surrounding materials, obstacles, etc.). Values of  $1.5 < n < 5.5$  have been reported in the literature, based on measurements [22]. See [22–24] for further reading and details.

### 3.1 Fading in Wireless Propagation Channels

Fading effects are the most important factors in signal fluctuation along the propagation channel. The propagation channel nature (direct sight, multipath, presence of obstacles and shadowing, reflection, scattering, etc.) causes that, at the receiver, the received signal strength fluctuates. The received signal is composed of multipath signals with randomly distributed amplitudes and phases, combined to give a resultant signal that varies in time and space [25]. In a real propagation channel, the received signal levels and the signal nature depend on the existence of line of sight (LOS scenario), or the absence of it on the contrary (NLOS scenario). Meanwhile in LOS scenarios the level of direct signal is higher compared to the rest of multipath versions of the propagated signal, in NLOS scenarios there is not a signal component which prevails in terms of amplitude over the rest of them.

The short-term fluctuation in the signal amplitude caused by the local multipath is called *small-scale fading*. Due to the effect of multipath, a receiver can experience several fades depending on its position. On the other hand, long-term variation in the mean signal level is called *large-scale fading*. Large-scale fading is also known as *shadowing*, because these variations in the mean signal level are caused by the presence of signal shadow areas due to surrounding elements in the propagation scenario. Small-scale fading may be further classified as flat or frequency selective, and slow or fast [22]. In real scenarios, fading effects become an issue of great concern for proper communication.

The most typical channel models are:

- (i) Large-scale fading: shadowing. The shadowing effect in propagation channels is frequently modeled with a distance-based loss model log-normal distribution [22]. The signal fluctuation due to shadowing is provided by a normal random variable in dB (log-normal in linear units), with a standard deviation of  $\sigma$  (dB), according to:

$$P_{R_x}(d) = P_{R_x_{d_0}} + 10n \log \left( \frac{d_0}{d} \right) + X_\sigma \quad (3)$$

Depending on the scenario properties, different values for the tuple  $[n, \sigma]$  are considered in (3). Typical values are  $4 \text{ dB} < \sigma < 10 \text{ dB}$  [22].

- (ii) Small-scale NLOS flat fading: Rayleigh model. If there is no line of sight (LOS) component, a Rayleigh distribution is observed in the received signal.
- (iii) LOS small-scale flat fading: Ricean model. The Ricean distribution is observed when, in addition to the multipath components, there exists a direct path between the transmitter and the receiver.
- (iv) Combined large-scale and small-scale fading: Suzuki model. This approach combines the Rayleigh and lognormal in a single model [26]. The resulting model combines

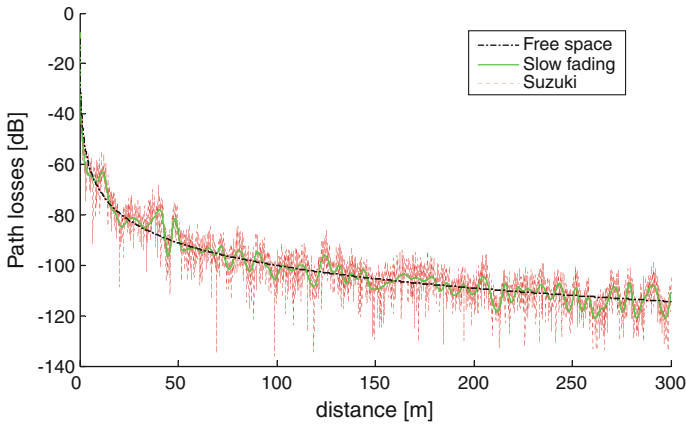


**Fig. 3** Suzuki fading effect in a NLOS indoor propagation channel with large scale and small scale fading, with  $\sigma = 3.4$  dB and  $n = 3$

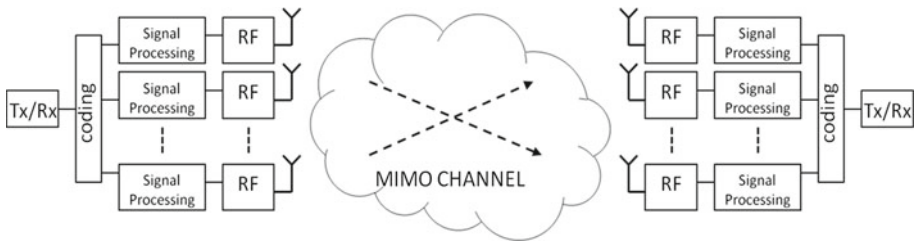


**Fig. 4** Conventional  $N \times N$  MIMO scheme

Rayleigh and log-normal distributions in the form of a Rayleigh distribution with a log-normally varying mean.

The probability distribution function (Pdf) of these channel models may be found in [23,24]. For the sake of clarity, Fig. 3 provides the fading effect in a NLOS indoor propagation channel with slow and fast fading, based on Suzuki model with  $\sigma = 3.4$  dB and  $n = 3$ .

### 3.2 Multiple Input Multiple Output (MIMO) and Terminal Gain

The increasing interest in MIMO systems has given rise to a prolific research activity in this topic in recent years [24]. Several aspects have been studied, regarding channel capacity and its enhancement. So far much effort has been put in the study and design of MIMO systems for communication systems, taking into account the previous knowledge of the type of scenario and channel features at the transmitter. MIMO systems performances depend on three aspects: number of antennas (spatial diversity), channel characteristics (frequency or time domain multiplexation) and coding (code domain multiplexation) [27]. Figure 4 shows a conventional  $N \times N$  MIMO scheme.

Many works can be found in the literature for a wide range of wireless communication systems [28]. Considering WSN and the necessity of low power consumption, only some issues of MIMO techniques may be considered and successfully developed. In this case of study only spatial diversity is considered, as it is the simplest option in terms of new RF



**Fig. 5**  $2 \times 2$  MIMO scheme considering only space diversity

or processing blocks needed and their derived consumption. In this work, a  $2 \times 2$  MIMO scheme including space diversity is considered as shown in Fig. 5. In this case, the power is split into both terminals and recombined at the receiver, ideally with no losses, actually with the losses associated to the splitter and combiner. In order to de-correlate channel signals from both terminals, a change in polarization may be selected. Thus, one of the paths may suffer a great fading meanwhile the complementary one may not.

In addition, in realistic scenarios, the antenna gain, radiation pattern and its features are topics of great concern. Although this radio issues are not matter of study in this work, some implications have to be considered. The antenna gain is a fundamental aspect when computing the channel link losses. Ideally, this antenna gain is considered to be fixed to a particular value. However, in real scenarios the antenna gain depends on the radiation direction and its value fluctuates in a defined range [ $G_{max}$ ,  $G_{min}$ ]. This gain variation is considered in all the scenarios proposed in this work.

## 4 Evaluation and Simulation Results

### 4.1 Evaluation Scenario

In order to evaluate the performance of the proposed energy-efficient routing algorithms, a simulation scenario is defined. In order to have a realistic approach, commercial MICAz devices are selected as a reference and their features are assumed, in terms of energy consumption, coverage, working frequency, transmission rate and bandwidth. Main features of this test scenario are summarized in Table 1.

Table 2 shows the different propagation channel models and the node configuration considered for each model. For the evaluation of the different proposed scenarios, MATLAB<sup>®</sup>

**Table 2** Propagation channel models

#### *Propagation channel and node configuration*

SC1	Free space losses, one Tx/Rx antenna with gain variation
SC2	Free space losses, MIMO scheme with two Tx/Rx antennas with gain variation
SC3	NLOS channel model with slow and fast fading, indoor scenario. One Tx/Rx antenna with gain variation
SC4	NLOS channel model with slow and fast fading, indoor scenario. MIMO scheme with two Tx/Rx antennas with gain variation



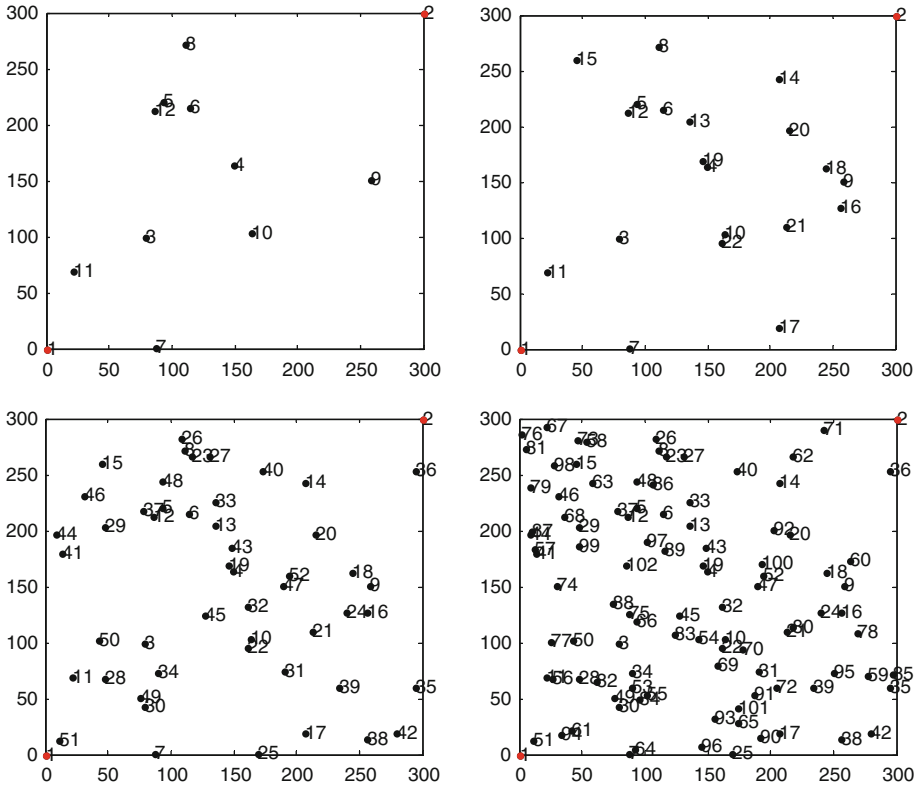


Fig. 6 Node evolution in one of the 100 randomly generated scenarios

has been selected as computational simulation tool. All the different propagation models, the node scenarios and all the computations and results have been obtained with MATLAB. Some details about the different propagation channel models and their implementation in MATLAB are found in [26].

According to the specifications previously given, the outcomes of the different routing algorithms are obtained, for a node-growing scenario. In order to have statistical confidence in the outcomes, the results are a compendium of 100 randomly generated scenarios. Figure 6 depicts the node evolution in one of the 100 random scenarios, for an increasing number of nodes. The source node (node 1) and the destination one (node 2) are located in the bottom left and top right corners, respectively.

Previous to any algorithm evaluation, the proper value of  $d_{opt}$  has to be calculated to fix  $A_{IN}$ ,  $A_{OUT}$  or the circle  $C$ , in Fig. 1. According to the formula derived from (1), in Table 1, an estimation of the optimum value of  $d_{opt}$  can be obtained. This optimum value is loss-factor ( $n$ ) dependent. Therefore, the nature of the evaluation scenario must be known in order to define a proper value. Figure 7 shows the evolution of  $d_{opt}$  for different  $n$  values:  $d_{opt}$  decreases when increasing  $n$ .

In the rest of this work a value of  $n = 3$  is assumed, and, as a consequence, a value of  $d_{opt} = 41$  m is set.

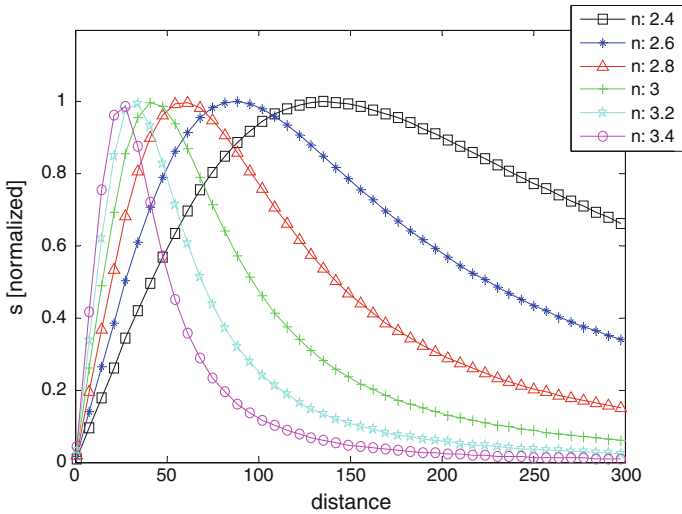


**Fig. 7** Evolution of  $d_{opt}$  for different  $n$  values

#### 4.2 Ideal Free Space Scenario

The most optimistic scenario is the one in which only the effects of free space propagation are considered (SC1, in Table 2). In this work, the simulation results obtained in this ideal scenario are considered as a baseline reference in order to evaluate the performance of the energy efficient routing algorithms and their evolution according to the variation in the propagation channel considered. Its performance results are provided in Fig. 8.

As it can be noticed, in the most optimistic scenario (only free space losses considered) the difference between the best route (Dijkstra) and *GeRaF*, *B\_Above*, *B\_Below*, and *EEGR* is lower than 1 dB. The last three algorithms improve their performance with the addition of nodes in the simulation until 50 nodes are included. For higher number of nodes, the improvement is negligible. On the other hand, *GeRaF* seems to improve its performance with the addition of nodes. For a high enough number of nodes, *GeRaF* outperforms the other three approaches, showing statistical significant differences ( $p$  value  $<0.01$ <sup>1</sup>) with the other approaches from 300 nodes or more. In addition, Fig. 8b shows the number of hops needed in each option to reach the destination node. In all the cases, the best-route reference establishes the lowest number of hops. Note that the best route (Dijkstra) approach provides the best route in terms of global power consumption.

The next scenario, SC2, consists of the same free space propagation model, with a  $2 \times 2$  MIMO Tx/Rx scheme and two Tx/Rx antennas with gain variation. The performance results obtained are shown in Fig. 9.

In average, this scenario is quite similar to SC1. The introduction of the additional propagation path of the  $2 \times 2$  MIMO scheme has only influence in the antenna gain fluctuation, which is different for each path. The  $2 \times 2$  MIMO configuration is not of influence in the propagation losses, which are assumed to be the same in both paths because of the only consideration of free space losses.

<sup>1</sup> Statistical significance checked through Analysis of Variance (ANOVA).

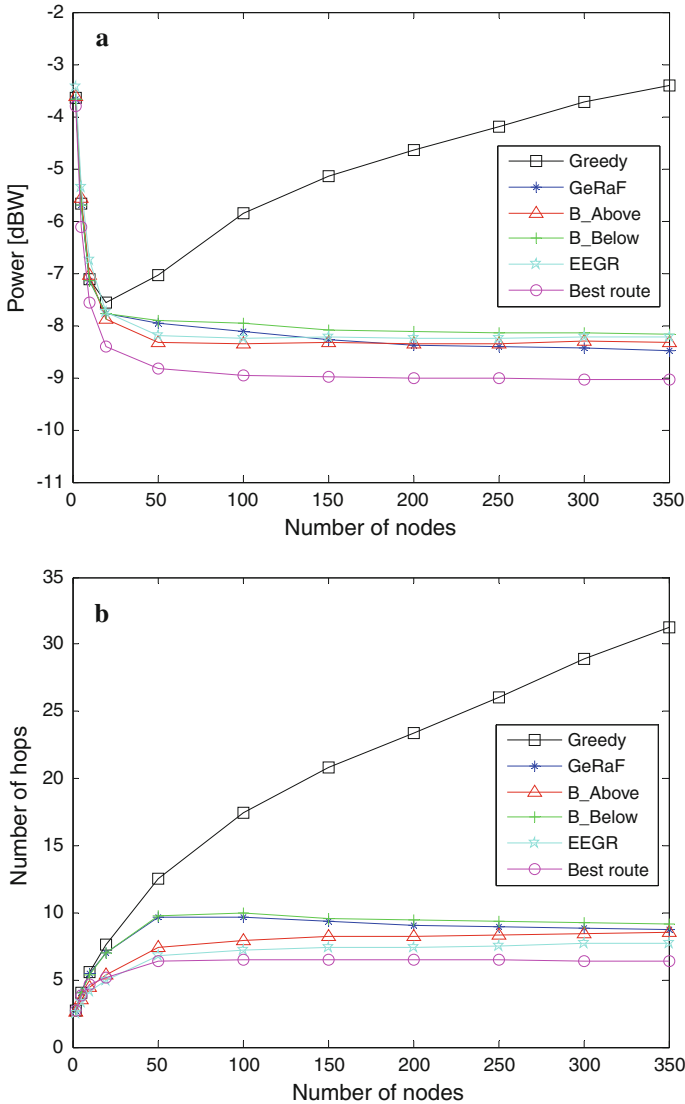


**Fig. 8** a Performance (global power consumption in the route) of the energy efficient routing algorithms and their evolution in SC1, b number of hops to reach the destination node

### 4.3 Impact of Propagation Factors

In the next scenario, SC3, a *NLOS* indoor channel model with large and small scale fading (Suzuki) and one Tx/Rx antenna with gain variation is considered. The performance results are shown in Fig. 10

The case in SC3 is the worst one because of the influence of large and small fading in propagation. In some hops, the combination of these effects may introduce an important propagation fading, being necessary a higher amount of power to reach the next node (compared

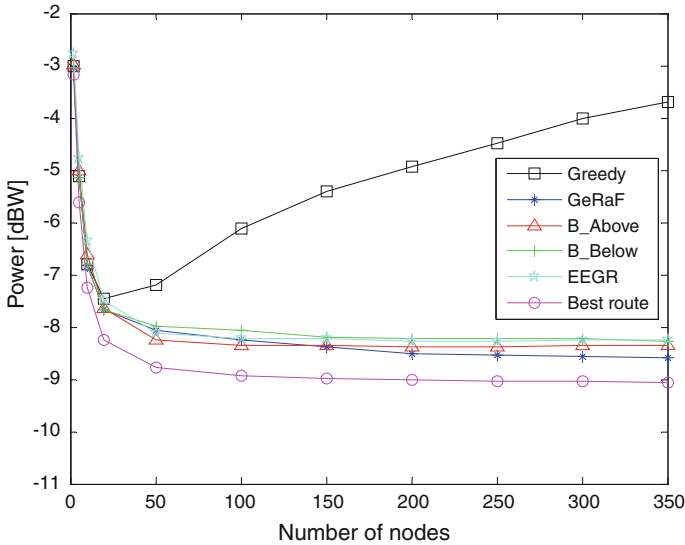


**Fig. 9** Performance (global power consumption in the route) of the energy efficient routing algorithms and their evolution in SC2

to SC2, about 0.65 dB). It is of particular relevance that the power necessities of the best-route option (Dijkstra) decay drastically in this scenario. This fact is due to the existence of hops between nodes where no signal fading but signal enhancement is found. This fact ideally establishes the highest level of possible improvement in power consumption in this scenario. SC3 is the most realistic case and the one in which a MIMO scheme would contribute more.

It should be noted that while the number of hops in SC3 (Fig. 10b) remains very similar to that of SC1 (Fig. 8b) the same does not happen with the performance in terms of energy. In Fig. 10a, *GeRaF* shows lower average energy consumption than *B\_Above*, *B\_Below*, and *EEGR* with statistical significant differences ( $p$  value  $< 0.01$ ) with the other approaches from 200 nodes or more. Comparing this result with the discussion of Fig. 8a illustrates that considering simplistic propagation models may lead to incorrect conclusions regarding energy consumption in both absolute and relative terms.

The last considered scenario, SC4, consists of a *NLOS* indoor channel model with large and small scale fading (Suzuki) and a  $2 \times 2$  MIMO scheme with two Tx/Rx antennas with gain variation (Fig. 11).

The comparison between SC3 and SC4 is of great interest, because of the reduction on the influence of propagation fading in the global performance of a complete node to node communication. Table 3 provides the comparison between both scenarios. Meanwhile the power needed in the best-route case is quite similar to the one in SC3, the reduction in needed power for the rest of the algorithms is of about 0.6 dB. Notice this improvement due to the use of a MIMO system is neither identified when a simplistic propagation scenario is considered.

#### 4.4 Effectiveness in the Selection of $d_{opt}$

According to the literature,  $d_{opt}$  is selected so that the power efficiency at each hop reaches its optimum. However, it may not be correct to assume that the best choice of  $d_{opt}$  at any hop leads to the optimum global power consumption in the complete network. The total efficiency

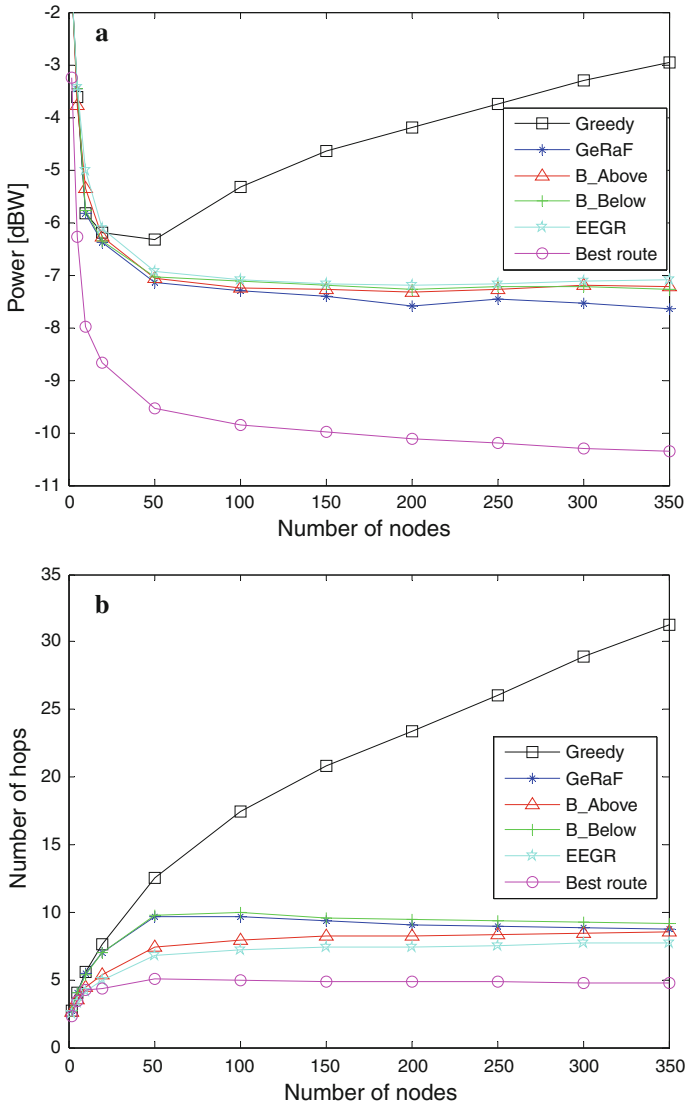


**Fig. 10** a Performance (global power consumption in the route) of the energy efficient routing algorithms and their evolution in SC3, b number of hops to reach the destination node

also depends on the number of hops: as it can be derived from the evaluation in Sect. 4, the best choice usually implies a reduced number of hops. This fact leads to the idea of oversizing a bit the value of  $d_{opt}$ , in order to determine if the global efficiency is improved. This supposition has been evaluated for 100, 200 and 300 nodes in the SC1 scenario, for *B\_Above*, *B\_Below*, *GeRaF* and *EEGR*, considering again the compendium of 100 randomly generated scenarios. The results are shown in Fig. 12.

As it can be shown, the distance value for  $d_{opt}$  which leads to the optimum global efficiency is a bit larger than the previously calculated value, mainly for *GeRaF* and *B\_Below*. The same tendency is found for the most demanding scenario SC3.

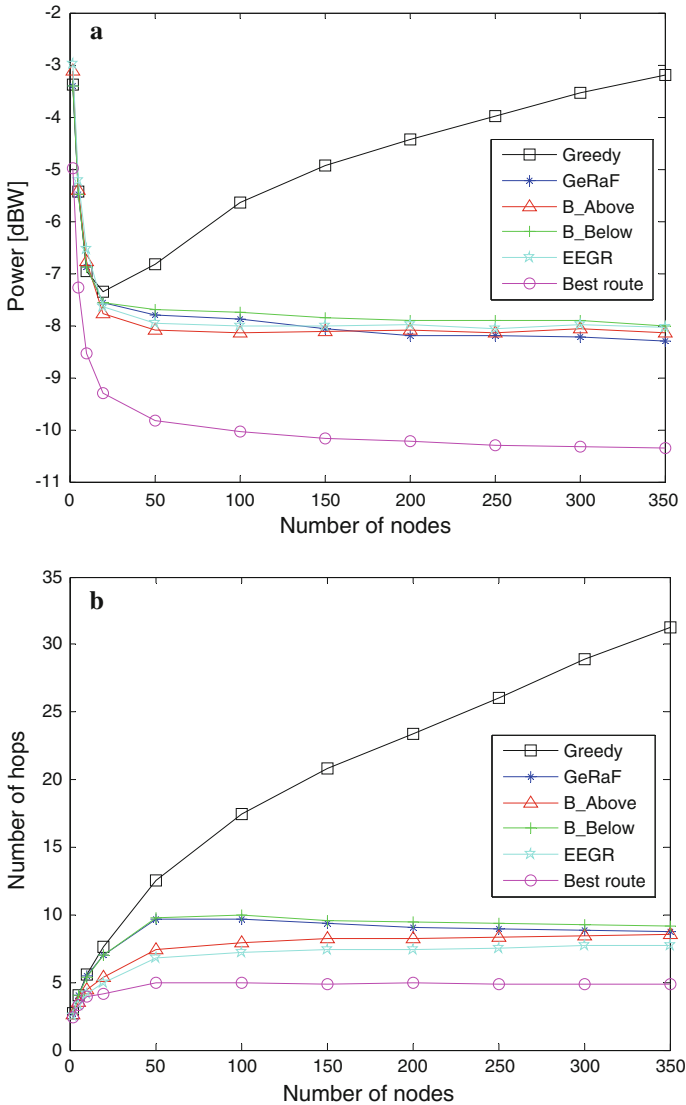


**Fig. 11** **a** Performance (global power consumption in the route) of the energy efficient routing algorithms and their evolution in SC4, **b** number of hops to reach the destination node

#### 4.5 Simulation Evaluation with Real Indoor Scenario Measurements

In order to complete the study of the performance of all these routing algorithms, it has been performed a simulation evaluation considering measurements in a real scenario for the path power balance between nodes. The real scenario consists of an indoor office building (dependencies of the Technical University of Madrid) analyzed with the  $2 \times 2$  dual-polarized MIMO test-bed UMAT (UPM Multi-Antenna Test-bed) [29], at 2.4GHz. Figure 13 presents the floormap of the office scenario. The blue dots are the points in which the measurements

**Table 3** Comparison between SC3 and SC4

	Number of nodes											
	2	5	10	20	50	100	150	200	250	300	350	
<i>Greedy</i>												
SC3 (dBW)	-11.7	-13.6	-15.8	-16.2	-16.3	-15.3	-14.7	-14.2	-13.8	-13.3	-13.0	
SC4 (dBW)	-13.4	-15.4	-17.0	-17.4	-16.8	-15.7	-14.9	-14.4	-14.0	-13.5	-13.2	
Diff (dB)	1.7	1.8	1.1	1.2	0.5	0.3	0.3	0.3	0.2	0.2	0.2	
<i>GeRaF</i>												
SC3 (dBW)	-11.6	-13.5	-15.8	-16.4	-17.1	-17.3	-17.4	-17.6	-17.5	-17.5	-17.6	
SC4 (dBW)	-13.4	-15.5	-16.9	-17.6	-17.8	-17.9	-18.1	-18.2	-18.2	-18.2	-18.3	
Diff (dB)	1.8	2.0	1.1	1.2	0.7	0.6	0.7	0.6	0.7	0.7	0.7	
<i>B_Above</i>												
SC3 (dBW)	-11.5	-13.8	-15.4	-16.3	-17.1	-17.2	-17.3	-17.3	-17.3	-17.2	-17.2	
SC4 (dBW)	-13.1	-15.4	-16.8	-17.8	-18.1	-18.2	-18.1	-18.1	-18.2	-18.1	-18.1	
Diff (dB)	1.6	1.6	1.4	1.5	1.0	0.9	0.8	0.8	0.9	0.9	0.9	
<i>B_Below</i>												
SC3 (dBW)	-11.6	-13.5	-15.8	-16.4	-17.0	-17.1	-17.2	-17.3	-17.2	-17.2	-17.3	
SC4 (dBW)	-13.4	-15.5	-16.9	-17.6	-17.7	-17.7	-17.9	-17.9	-17.9	-17.9	-18.0	
Diff (dB)	1.8	2.0	1.1	1.2	0.7	0.6	0.7	0.6	0.7	0.7	0.7	
<i>EEGR</i>												
SC3 (dBW)	-11.3	-13.4	-15.0	-16.1	-16.9	-17.1	-17.2	-17.2	-17.2	-17.1	-17.1	
SC4 (dBW)	-13.0	-15.2	-16.5	-17.6	-18.0	-18.0	-18.0	-18.0	-18.1	-18.0	-18.0	
Diff (dB)	1.7	1.8	1.5	1.5	1.0	0.9	0.8	0.8	0.9	0.9	1.0	
<i>Dijkstra</i>												
SC3 (dBW)	-13.3	-16.3	-18.0	-18.7	-19.5	-19.8	-20.0	-20.1	-20.2	-20.3	-20.4	
SC4 (dBW)	-15.0	-17.3	-18.5	-19.3	-19.8	-20.0	-20.2	-20.2	-20.3	-20.3	-20.4	
Diff (dB)	1.7	1.0	0.5	0.6	0.3	0.2	0.2	0.1	0.1	0.0	0.0	

Table 3 continued

	Number of nodes											
	2	5	10	20	50	100	150	200	250	300	350	
<i>SC3</i>												
Greedy versus Dijkstra (dB)	1.5	2.7	2.1	2.5	3.2	4.5	5.3	5.9	6.5	7.0	7.4	
<i>GeRaF</i> versus Dijkstra (dB)	1.6	2.8	2.2	2.3	2.4	2.5	2.6	2.5	2.7	2.8	2.7	
Bound-Above versus Dijkstra (dB)	1.8	2.5	2.6	2.4	2.5	2.6	2.7	2.8	2.9	3.1	3.1	
Bound-Below versus Dijkstra (dB)	1.6	2.8	2.2	2.3	2.5	2.7	2.8	2.8	3.0	3.1	3.1	
<i>EEGR</i> versus Dijkstra (dB)	1.9	2.8	3.0	2.6	2.6	2.8	2.8	2.9	3.0	3.2	3.3	
<i>SC4</i>												
Greedy versus Dijkstra (dB)	1.6	1.8	1.6	2.0	3.0	4.4	5.3	5.8	6.3	6.8	7.2	
<i>GeRaF</i> versus Dijkstra (dB)	1.6	1.8	1.7	1.8	2.0	2.2	2.1	2.0	2.1	2.1	2.0	
Bound-Above versus Dijkstra (dB)	1.9	1.8	1.7	1.5	1.7	1.9	2.1	2.1	2.2	2.2	2.2	
Bound-Below versus Dijkstra (dB)	1.6	1.8	1.7	1.8	2.1	2.3	2.3	2.3	2.4	2.4	2.4	
<i>EEGR</i> versus Dijkstra (dB)	2.0	2.0	2.0	1.7	1.9	2.0	2.2	2.2	2.3	2.3	2.3	



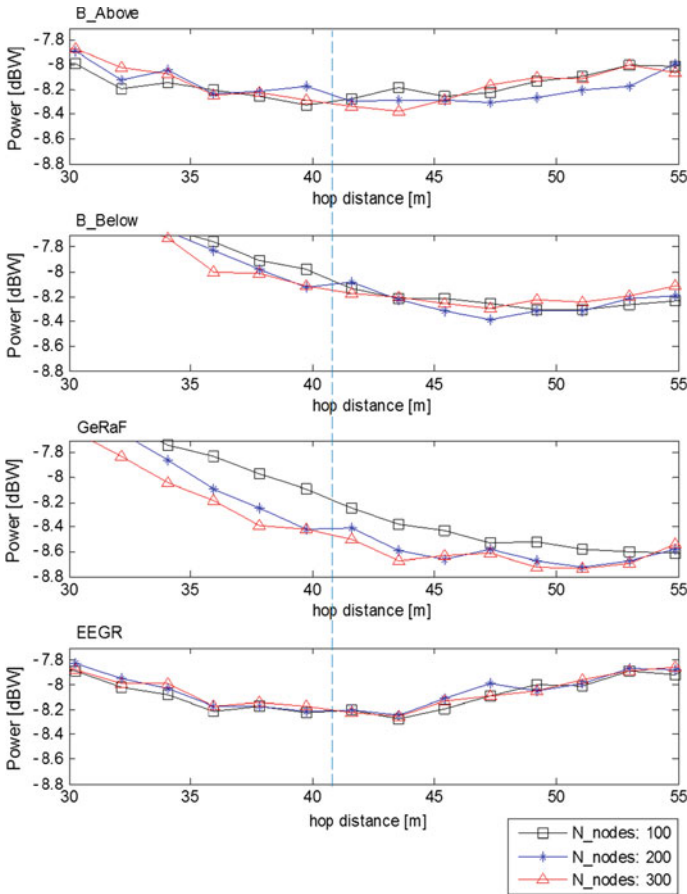


**Fig. 12** Evolution of  $d_{opt}$ , regarding the number of nodes, for *B\_Above*, *B\_Below*, *GeRaF* and *EEGR* in SC1

were taken (105 points separated 2 m from the next dots of the grid). Thus 20,050 measurements are carried out, for the 2-channel propagation scenario ( $105 \times 105 \times 2$ ), yielding the propagation matrix of the scenario.

This simulation evaluation consists of 100 node-growing scenarios with the nodes randomly placed in the positions shown in Fig. 13. In all of these scenarios, the needed power from one node to reach other is obtained from the measured  $2 \times 2$  propagation matrix. Thus, energy consumption results are based on real measurements. For the sake of completeness, it can be also computed that the measured propagation matrix yields an equivalent propagation factor of  $n \approx 3.2$  and  $\sigma \approx 2.7$  dB.

In this evaluation, the power efficiency of the above-mentioned routing algorithms is evaluated and the results are offered in Fig. 14. In the evaluation, the number of working nodes is increased from 2 nodes, up to 90 and their locations are randomly selected among the available measurement locations in the real scenario. Origin and destination nodes are placed in locations 1 and 105, respectively. As mentioned, 100 scenarios with randomly placed nodes (uniform distribution) are evaluated and their average performance results are provided in Fig. 14.

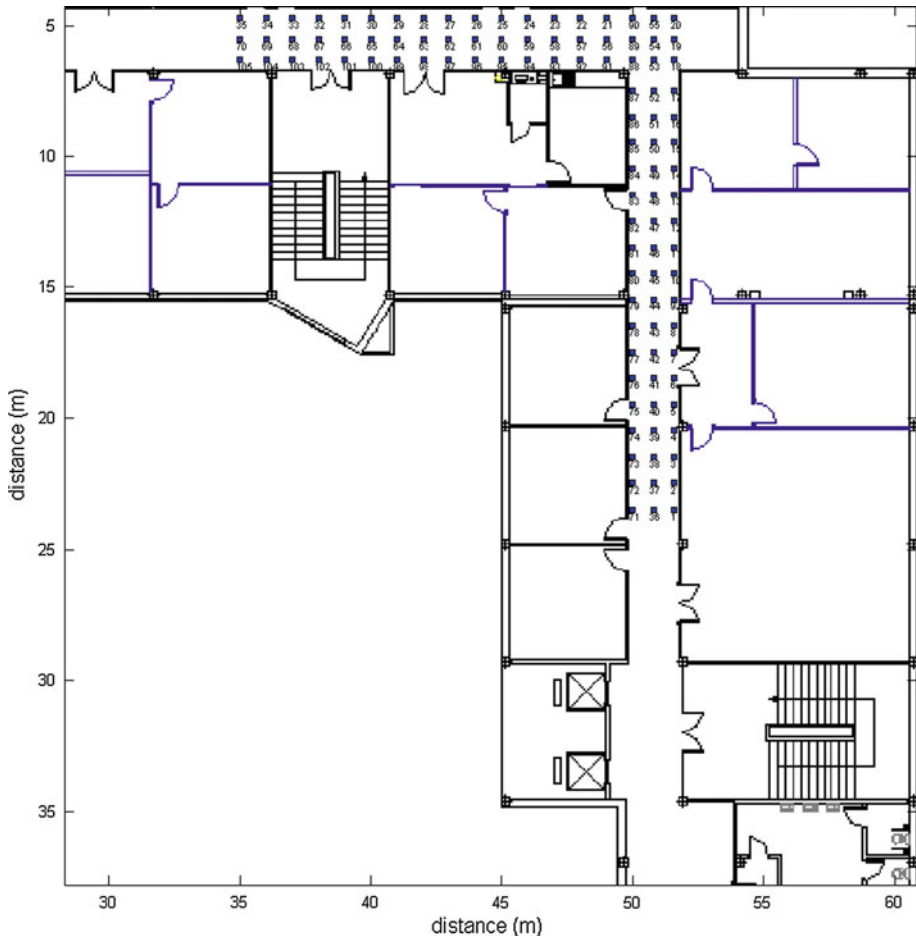


**Fig. 13** Floormap of the real indoor scenario

According to (A.3) the value of  $d_{opt}$  in this case is around 31 m. As it can be seen, the results are similar to the ones in SC4. Although the performance of  $B\_Above$  or  $EEGR$  is better than the one of the rest for a low number of nodes, the tendency of evolution is quite similar to the one in SC4 for a more populated scenario. The evaluation with the measurements obtained in the real scenario lets validate both, the algorithms behavior and the tendency of evolution which is quite similar to the one in SC4, for instance, and it also lets validate the power levels obtained in the previous simulations.

## 5 Conclusion

In this paper, the influence of the nature of the propagation channel in the performance of WNS is studied. Although there are a lot of works regarding energy-efficient routing protocols, almost no reference to realistic propagation channel models and possible influence is made on them. In this work, different scenarios have been considered, from simple free space

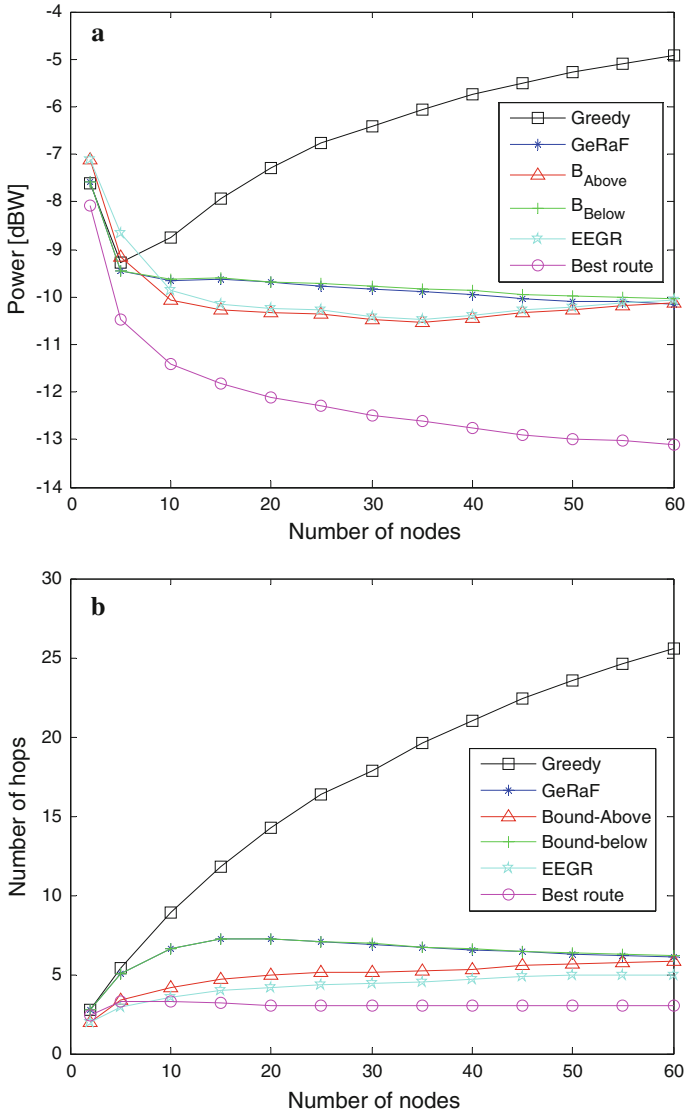


**Fig. 14** **a** Performance (global power consumption in the route) of the energy efficient routing algorithms and their evolution in the real indoor scenario, **b** number of hops to reach the destination node

propagation model to more complex Rayleigh multipath loss scenarios. Results illustrate the potential pitfalls of using a simplistic propagation model for routing algorithms evaluation. In addition, the influence of the system configuration is also tested, either considering simple transmission/reception chains or more elaborated  $2 \times 2$  MIMO communication configurations with spatial diversity. Valuable results are found when comparing the ideal case with an indoor *NLOS* channel model with large scale and small scale fading and one transmission/reception chain in the transmitter/receiver, as the performance of the energy-efficient routing algorithms decays. In addition, the comparison between the last scenario and its

equivalent scenario considering  $2 \times 2$  MIMO reveals that the effects of hostile environments may be mitigated by these kinds of configurations. In all the scenarios, most efficient approach implies a reduced number of hops needed to reach the destination, and must be taking into account when defining new routing algorithms. Throughout this paper, comparison between different scenarios with different assumptions is offered and discussed. Finally, for the sake of completeness, a performance evaluation in a real indoor scenario is provided.

**Acknowledgments** This work has been supported by the Spanish Government (Comisión Interministerial de Ciencia y Tecnología) under the “SuMA” project (REF: TEC2011-22579).

### Appendix

The calculation of the optimum distance  $d_{opt}$  is derived from the evaluation on the power consumption in one hop. Two factors are directly implied in this computation: the advancement in terms of distance and the power consumption joined to this advance. Figure 15 illustrates this fact.

Thus, the *advance* ratio  $s$  may be defined as:

$$s = \frac{d_{ij}}{P_{Tx_{ij}} + 2P_{elect}} \rightarrow \frac{\partial s}{\partial d_{ij}} = 0 \rightarrow d_{opt} \tag{A.1}$$

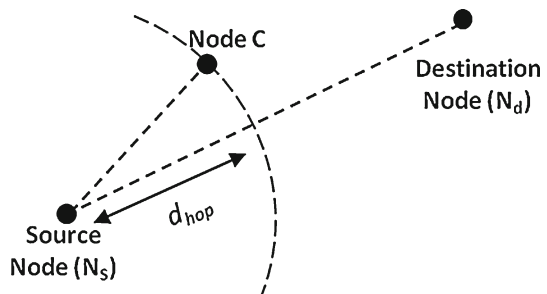
The complete formulation of  $s$  must consider the baseline loss model, without ripples and fluctuations, according to (2), defined as follows:

$$s = \frac{d_{hop}}{\left(\frac{4\pi}{\lambda}\right)^2 d_0^{(2-n)} d_{hop}^n \frac{S}{g_{Tx} g_{Rx}} + 2P_{elect}} \tag{A.2}$$

where  $d_0$  is a reference distance (see Sect. 3),  $S$  is the sensitivity of the receiver, and  $g_{Tx}$  and  $g_{Rx}$  are the transmitter and receiver gains (all the values in linear units). The optimization of  $s$  yields the optimum value of  $d_{opt}$ :

$$d_{opt} = \sqrt[n]{\frac{2P_{elect}\lambda^2}{4\pi^2 d_0^{(2-n)} (n-1) \frac{S}{g_{Tx} g_{Rx}}}} \tag{A.3}$$

**Fig. 15** Node topology to determine the optimum hop distance

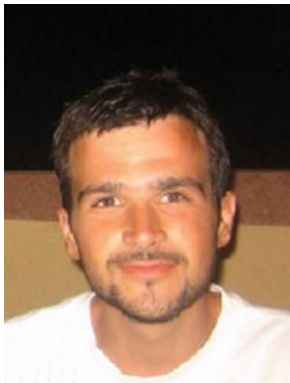


## References

1. Akyildiz, I. F., Su, W., Sankarasubramaniam, Y., & Cayirci, E. (2002). Wireless sensor networks: A survey. *Computer Networks*, 38(4), 393–422.
2. Anastasi, G., Conti, M., Di Francesco, M., & Passarella, A. (2009). Energy conservation in wireless sensor networks: A survey. *Ad Hoc Networks*, 7(3), 537–568.
3. Akkaya, K., & Younis, M. (2005). A survey on routing protocols for wireless sensor networks. *Ad Hoc Networks*, 3(3), 325–349.
4. Akyildiz, I. F., & Kasimoglu, I. H. (2004). Wireless sensor and actor networks: Research challenges. *Ad Hoc SNetworks*, 2, 351–367.
5. Akyildiz, I. F., Wang, X., & Wang, W. (2005). Wireless mesh networks: A survey. *Computer Networks*, 47(4), 445–487.
6. Mauve, M., Widmer, A., & Hartenstein, H. (2001). A survey on position-based routing in mobile ad hoc networks. *IEEE Network*, 15(6), 30–39.
7. Peng, B., & Kemp, A. H. (2011). Energy-efficient geographic routing in the presence of localization errors. *Computer Networks*, 55(3), 21, 856–872.
8. Mao, G., Fidan, B., & Anderson, B. D. O. (2007). Wireless sensor network localization techniques. *Computer Networks*, 51(10), 2529–2553.
9. Seada, K., Zuniga, M., Helmy, A., & Krishnamachari, B. (2004). Energy-efficient forwarding strategies for geographic routing in lossy wireless sensor networks. In *Proceedings of the 2nd international conference on Embedded networked sensor systems (SenSys '04)*, New York, NY, USA: ACM (pp. 108–121).
10. Zorzi, M., Casari, P., Baldo, N., & Harris, A. (2008). Energy-efficient routing schemes for underwater acoustic networks. *IEEE Journal on Selected Areas in Communications*, 26(9), 1754–1766.
11. Matrouk, K., & Landfeldt, B. (2009). RETT-gen: A globally efficient routing protocol for wireless sensor networks by equalising sensor energy and avoiding energy holes. *Ad Hoc Networks*, 7(3), 514–536.
12. Jin, Y., Jo, J., Wang, L., Kim, Y., & Yang, X. (2008). ECCRA: An energy-efficient coverage and connectivity preserving routing algorithm under border effects in wireless sensor networks. *Computer Communications*, 31(10), 2398–2407.
13. Lattanzi, E., Regini, E., Acquaviva, A., & Bogliolo, A. (2007). Energetic sustainability of routing algorithms for energy-harvesting wireless sensor networks. *Computer Communications*, 30(14–15), 2976–2986.
14. Abdulla, A., Nishiyama, H., & Kato, N. (2011). Extending the lifetime of wireless sensor networks: A hybrid routing algorithm. *Computer Communications*. Available online October 15, 2011.
15. Zorzi, M., & Rao, R. R. (2003). Geographic random forwarding (GeRaF) for ad hoc and sensor networks: Multihop performance. *IEEE Transactions on Mobile Computing*, 2(4), 337–348.
16. Abdallah, A. E., Fevens, T., Opatrny, J., & Stojmenovic, I. (2010). Power-aware semi-beaconless 3D georouting algorithms using adjustable transmission ranges for wireless ad hoc and sensor networks. *Ad Hoc Networks*, 8(1), 15–29.
17. Papadopoulos, A., Navarra, A., McCann, J. A., & Pinotti, C. M. (2011). VIBE: An energy efficient routing protocol for dense and mobile sensor networks. *Journal of Network and Computer Applications*. Available online May 24, 2011.
18. Alotaibi, E., & Mukherjee, B. (2011) A survey on routing algorithms for wireless ad-hoc and mesh networks. *Computer Networks*. Available online November 15, 2011.
19. Vazifehdan, J., Prasad, R. V., Onur, E., & Niemegeers, I. (2011). Energy-aware routing algorithms for wireless ad hoc networks with heterogeneous power supplies. *Computer Networks*, 55(15), 3256–3274.
20. Zhang, H., & Shen, H. (2007). EEGR: Energy-efficient geographic routing in wireless sensor networks. In *International Conference on Parallel Processing, ICPP 2007*.
21. Stojmenovic, I., Nayak, A., Kuruvila, J., Ovalle-Martinez, F., & Villanueva-Pena, E. (2005). Physical layer impact on the design and performance of routing and broadcasting protocols in ad hoc and sensor networks. *Computer Communications*, 28(10), 1138–1151.
22. Rappaport, T. (2002). *Wireless communications: Principles and practice* (2nd ed.). Englewood Cliffs, NJ: Prentice-Hall.
23. Molisch, A. F. (2005). *Wireless communications*. London: Wiley–IEEE press.
24. Goldsmith, A. (2004). *Wireless communications*. Cambridge: Cambridge University Press.
25. Prabhu, G. S., & Shankar, P. M. (2002). Simulation of flat fading using MATLAB for classroom instruction. *IEEE Transactions on Education*, 45(1), 19–25.
26. Pérez Fontán, F., & Mariño Espiñeira, P. (2008). *Modeling the wireless propagation channel: A simulation approach with MATLAB*. Wiley series on wireless communications and mobile computing.

27. Gomez-Calero, C., Cuellar, L., de Haro, L., & Martinez, R. (2011). A  $2 \times 2$  MIMO DVB-T2 system: Design, new channel estimation scheme and measurements with polarization diversity. *IEEE Transactions on Broadcasting*, 57(2), 195–203.
28. Gesbert, D., Shafi, M., Shiu, D. S., Smith, P., & Naguib, A. (2003). From theory to practice: An overview of MIMO space-time coded wireless systems. *IEEE Journal on Selected Areas in Communications*, 21(3), 281–302.
29. Gomez-Calero, C., Garcia-Garcia, L., de Haro-Ariet, L. (2006). New test-bed for evaluation of antenna and system performance for MIMO systems. In *First European Conference on Antennas and Propagation, EuCAP 2006*.

## Author Biographies



**P. Padilla** was born in Jaén in 1982. He received the Telecommunication Engineer degree from Technical University of Madrid (UPM), Spain, in 2005. Until September 2009, he was with the Radiation Group of the Signal, Systems and Radiocommunications Department of UPM, where he carried out his Ph.D. In 2007, he was with the Laboratory of Electromagnetics and Acoustics at Ecole Polytechnique Fédérale de Lausanne (EPFL), Switzerland, as an invited Ph.D. Student. In 2009 he carried out a postdoctoral stay at Helsinki University of Technology (AALTO-TKK). Nowadays, he is Associate Professor at Universidad de Granada (UGR). His research interests include a variety areas of knowledge, related to communication topics (radiofrequency devices, antennas, propagation), network topics (wireless communication networks), and data exploration topics.



**J. Camacho** is Associate Professor at the Department of Signal Theory, Telematics and Communications of the University of Granada (Spain). He holds a degree in Computer Science from the University of Granada (2003) and a Ph.D. in Control Systems and Industrial Computing from the Technical University of Valencia (2007). His Ph.D. was awarded with the second Rosina Ribalta Prize to the best Ph.D. projects in the field of Information and Communication Technologies (ICT) from the EPSON Foundation, and with the D.L. Massart Award in Chemometrics from the Belgian Chemometrics Society. His research interests include exploratory data analysis, monitoring, control and optimization with multivariate data analysis techniques. He has been principal author of more than 30 research articles and conference contributions and reviewer in more than 6 international journals.



**G. Maciá-Fernández** received the M.S. degree in telecommunications engineering from the University of Seville, Spain, and the Ph.D. degree in telecommunications engineering from the University of Granada, Spain. He is Associate Professor in the Department of Signal Theory, Telematics and Communications, University of Granada. From 1999 to 2005, he worked as a specialist consultant at “Vodafone Spain,” where he was involved in several research projects. His research was initially focused on multicasting technologies but he is currently working on computer and network security, with special focus on intrusion detection, reliable protocol design, and denial of service.



**J. E. Díaz-Verdejo** received the B.Sc. degree in physics (electronics speciality) from the University of Granada, Spain, in 1989, and the Ph.D. degree in physics in 1995. He is Full Professor in the Department of Signal Theory, Telematics and Communications, University of Granada, and member of the research group “Network Security and Engineering Group (NESG)”. His initial research interest was related with speech technologies, especially automatic speech recognition. Currently he is working in computer networks, mainly in computer and network security, although he has developed some work in telematics applications and e-learning systems.



**P. García-Teodoro** received the B.Sc. degree in physics (electronics speciality) from the University of Granada, Spain, in 1989. In 1989, he received a grant from “Fujitsu Spain,” and during 1990, he received a grant from “IBM Spain.” From 1989 to 2011, he was Associate Professor and, since 2011, Full Professor in the Department of Signal Theory, Telematics and Communications, University of Granada, and head of the research group “Network Security and Engineering Group (NESG)” of this University. His initial research interest was concerned with speech technologies, in which he developed his Ph.D. thesis in 1996. Since then, his professional interests have been in the field of computer and network security, especially focused on intrusion detection and denial of service attacks.



**C. Gómez-Calero** was born in Madrid, Spain, in 1981. He received the Ingeniero Técnico de Telecomunicación degree, the Ingeniero de Telecomunicación degree and the Doctor Ingeniero de Telecomunicación degree (cum laude), from Universidad Politécnica de Madrid, in 2002, 2005 and 2009, respectively. In 2003 he joined to the Radiation Group of the Signals, Systems and Radiocommunications department in UPM as a researcher. His research interests are in the areas of smart antennas, telecommunication systems, and mobile and satellite communications. Dr. Calero received the award to “The Best Master Thesis in Radiocommunications” from Rohde and Schwarz in 2003. He received in 2005 in Newport (USA) “The Best Student Paper Award” in 2005 AMTA Symposium. In 2007 he received the Foundation VODAFONE Award to the “Best Master Thesis in Advanced Mobile Communications”, and the RESA award to the “Best Paper in Antennas and Propagation” in XXII URSI Symposium.